phenotype in tissues other than the stem and leaf and accumulation of residual surface wax on the stem of *cer5-2* knockout line suggest that additional wax export mechanisms must exist in plants. Chemical analysis of the mutant wax demonstrated that CER5, like many ABC transporters, has broad substrate specificity and is capable of transporting a variety of wax substrates. We conclude that in plants, as in other eukaryotes, proteins of the WBC/ABCG subfamily are key components of lipid transport systems.

References and Notes

1. L. Kunst, A. L. Samuels, *Prog. Lipid Res.* **42**, 51 (2003).
2. M. Koornneef, C. J. Hanhart, F. Thiel, *J. Hered.* **80**, 118 (1989).
3. Materials and methods are presented as supporting material on *Science* Online.
4. H. Powell, R. Tindall, P. Schultz, *Arch. Neurol.* **32**, 250 (1975).
5. A. M. Rashotte, M. A. Jenks, K. A. Feldmann, *Phytochemistry* **57**, 115 (2001).
6. ABC transporter motifs were predicted by PROSITE as referenced in (*13*).
7. M. Jasinski, E. Ducos, E. Martinoia, M. Boutry, *Plant Physiol.* **131**, 1169 (2003).
8. R. Sánchez-Fernández, T. G. E. Davies, J. O. D. Coleman, P. A. Rea, *J. Biol. Chem.* **276**, 30231 (2001).
9. C. T. Otsu *et al.*, *J. Exp. Bot.* **55**, 1643 (2004).
10. The analyses of R. Sánchez-Fernández *et al.* (*8*) agree with these relationships; however, they erroneously duplicated WBC15/WBC22 in their 2001 work. This was corrected in (*14*).
11. G. L. Scheffer *et al.*, *Cancer Res.* **60**, 2589 (2000).
12. J. W. Jonker *et al.*, *Proc. Natl. Acad. Sci. U.S.A.* **99**, 15649 (2002).
13. L. Falquet *et al.*, *Nucleic Acids Res.* **30**, 235 (2002).
14. P. A. Rea *et al.*, in *ABC Transporters from Bacteria to Man*, I. B. Holland, S. P. C. Cole, K. Kuchler, C. F. Higgins, Eds. (Academic Press, London, 2003), pp. 335–355.

15. Thanks to G. Haughn, M. Smith, T. Hooker, and O. Rowland for their insightful comments. The financial support of the Natural Sciences and Engineering Research Council of Canada, Canadian Foundation for Innovation, BC Knowledge Development Foundation, and the UBC Blusson fund are gratefully acknowledged. We thank the Salk Institute for Genomic Analysis Laboratory for providing sequence-indexed *Arabidopsis* T-DNA insertion mutants (project funded by NSF). The *CER5* gene has been submitted to Genbank, and the accession no. is AY734542.

Supporting Online Material

www.sciencemag.org/cgi/content/full/306/5696/702/DC1
Materials and Methods
Figs. S1 to S4

5 July 2004; accepted 3 September 2004

Oscillations in NF-κB Signaling Control the Dynamics of Gene Expression

D. E. Nelson,[1] A. E. C. Ihekwaba,[2] M. Elliott,[1] J. R. Johnson,[1] C. A. Gibney,[1] B. E. Foreman,[1] G. Nelson,[1] V. See,[1] C. A. Horton,[1] D. G. Spiller,[1] S. W. Edwards,[1] H. P. McDowell,[4] J. F. Unitt,[5] E. Sullivan,[6] R. Grimley,[7] N. Benson,[7] D. Broomhead,[3] D. B. Kell,[2] M. R. H. White[1]*

Signaling by the transcription factor nuclear factor kappa B (NF-κB) involves its release from inhibitor kappa B (IκB) in the cytosol, followed by translocation into the nucleus. NF-κB regulation of IκBα transcription represents a delayed negative feedback loop that drives oscillations in NF-κB translocation. Single-cell time-lapse imaging and computational modeling of NF-κB (RelA) localization showed asynchronous oscillations following cell stimulation that decreased in frequency with increased IκBα transcription. Transcription of target genes depended on oscillation persistence, involving cycles of RelA phosphorylation and dephosphorylation. The functional consequences of NF-κB signaling may thus depend on number, period, and amplitude of oscillations.

NF-κB is a family of dimeric transcription factors (usually RelA/p65:p50) that regulates cell division, apoptosis, and inflammation (*1*). NF-κB dimers are sequestered in the cytoplasm of unstimulated cells by binding to IκB proteins. NF-κB–activating stimuli activate the inhibitor kappa B kinase (IKK) signalosome that phosphorylates IκB [at Ser32 and Ser36 on IκBα (*2*)] and NF-κB [at Ser536 in RelA (*3*, *4*)]. Phosphorylated IκB proteins are then ubiquitinated and degraded by the proteasome, liberating NF-κB dimers to translocate to the nucleus and regulate target gene transcription.

IκBα is a transcriptional target for NF-κB (*5*), creating a negative feedback loop (Fig. 1A) in which its delayed expression gives the system similar characteristics to the circadian clock (*6*) and to ultradian oscillators such as p53 (*7*, *8*) and the segmentation clock (*8*, *9*). IκBα contains both nuclear localization and export sequences, enabling its nuclear-cytoplasmic (N-C) shuttling. Newly synthesized free IκBα binds to nuclear NF-κB, leading to export of the complex to the cytoplasm (*10*). This complex, but not free IκBα, is the target for IκBα phosphorylation by IKK (*11*, *12*).

Oscillations in the temporal response of NF-κB activity have been observed by electromobility shift assay (EMSA) only in studies of IκBβ and ε knockout mouse embryonic fibroblast cell populations and have been simulated in a computational model (*13*). In the absence of time-lapse single-cell analysis, it has remained unclear whether asynchronous single-cell oscillations occur in single cells following NF-κB stimulation (*8*, *14*). Like calcium signaling (*15*), NF-κB could be a complex dynamic oscillator using period and/or amplitude to regulate transcription of target genes.

We have used fluorescence imaging of NF-κB (RelA) and IκBα fluorescent fusion proteins (*11*, *16*) to study oscillations in RelA N-C localization (N-C oscillations) in HeLa (human cervical carcinoma) cells and SK-N-AS cells [human S-type neuroblastoma cells that have been associated with deregulated NF-κB signaling (*17*)]. In SK-N-AS cells expressing RelA fused at the C terminus to the red fluorescent protein DsRed (RelA-DsRed) and IκBα fused at the C terminus to the enhanced green fluorescent protein EGFP (IκBα-EGFP) (Fig. 1B and Fig. 2A), 96% showed an NF-κB nuclear translocation response to tumor necrosis factor alpha (TNFα) stimulation and 72% showed long-term N-C oscillations in RelA-DsRed localization. Oscillations with a typical period of ~100 min continued for >20 hours after continuous TNFα stimulation, damping slowly. In transfected cells expressing RelA-DsRed and control EGFP (Fig. 2C), 97% responded and 91% of cells showed N-C oscillations. These oscillations appeared more synchronous between cells in the first three cycles

[1]Centre for Cell Imaging, School of Biological Sciences, Bioscience Research Building, Crown Street, Liverpool, L69 7ZB, UK. [2]Department of Chemistry, [3]Department of Mathematics, University of Manchester Institute of Science and Technology, P.O. Box 88, Sackville Street, Manchester, M60 1QD, UK. [4]Royal Liverpool Children's National Health Service Trust, Alder Hey Hospital, Eaton Road, Liverpool, L12 2AP, UK. [5]Molecular Biology Department, [6]Advanced Science and Technology Laboratory, AstraZeneca Research and Development Charnwood, Bakewell Road, Loughborough, Leicestershire, LE11 5RH, UK. [7]Pfizer Central Research, Ramsgate Road, Sandwich, Kent, CT13 9NJ, UK.

*To whom correspondence should be addressed. E-mail: mwhite@liv.ac.uk

compared with cells that also expressed IκBα-EGFP, which suggests that the system was sensitive to variation in IκBα levels, thus contributing to the degree of cell-to-cell asynchrony. When HeLa cells were continually stimulated with TNFα (Fig. 2D), 86% of the cells responded and 30% exhibited up to three detectable N-C oscillations that were markedly damped. However, when TNFα was added to SK-N-AS cells (Fig. 2B) or HeLa cells (Fig. 2E) as a 5-min pulse, a single peak of nuclear occupancy was observed with no subsequent cycles of RelA movement.

TNFα treatment induced endogenous RelA localization patterns in cells, consistent with increasingly asynchronous N-C oscillations (fig. S3). Western blot analysis (figs. S4 and S5) showed that SK-N-AS and HeLa cells continually treated with TNFα gave biphasic dynamics of total IκBα, phosphorylated IκBα (Ser32 phospho-IκBα), and phosphorylated RelA (Ser536 phospho-RelA). In HeLa cells, phosphoprotein expression levels diminished more rapidly than in the SK-N-AS cells (fig. S5). A 5-min TNFα pulse directed transient accumulation of Ser32 phospho-IκBα and Ser536 phospho-RelA (fig. S4B). These data support the hypothesis that loss of IKK activity (due to TNFα removal) results in loss of N-C oscillations and that dephosphorylation of RelA occurs rapidly without persistent IKK activity. When SK-N-AS cells were treated with an alternative stimulus, the topoisomerase II inhibitor etoposide (VP16), 37% of the cells responded and 24% showed N-C oscillations. Etoposide-induced N-C oscillations had lower amplitude than those induced by TNFα, peaking after 300 min and then diminishing (Fig. 2F). The IκBα and RelA phosphoprotein expression levels after etoposide treatment (fig. S4C) corresponded to the timing of N-C oscillations.

We investigated whether N-C oscillation persistence influenced the dynamics of NF-κB–regulated gene expression using real-time imaging of firefly luciferase activity (*18*) driven by a κB (5× consensus site) promoter. SK-N-AS cells exhibited stable luminescence for more than 25 hours in the continual presence of TNFα (Fig. 2G). HeLa cells showed a transient peak 10 hours after TNFα treatment that decayed by 20 hours (Fig. 2I). In SK-N-AS (Fig. 2H) or HeLa cells (Fig. 2J) treated with a 5-min TNFα pulse, a more transient peak of luminescence occurred after 5 hours, which decayed by 10 hours. Etoposide treatment of SK-N-AS cells elicited a lower luminescence signal, reaching a peak at ~15 hours after treatment (Fig. 2K). With each stimulus, the kinetics of NF-κB oscillations and maintenance of phosphoprotein levels appeared closely related to the kinetics of gene expression. Thus, persistent NF-κB oscillations appear to maintain NF-κB–dependent gene expression.

Analysis of successive peaks of RelA nuclear occupancy (figs. S13 and S14 and Fig. 3, E and F) showed that N-C oscillation damping and successive peak timing were highly reproducible, but because of phase differences, this was not apparent at the population level. However, the pattern of peak timing and amplitudes was different between HeLa and SK-N-AS cells. The expression of IκBα–EGFP affected the amplitude and peak timing of the N-C oscillations (fig. S14). To study the role of IκBα synthesis rate on N-C oscillations, the rate of NF-κB–regulated IκBα transcription was modulated. IκBα-EGFP expression was driven by the κB (5× consensus site) promoter and expressed in HeLa cells together with a fusion protein between RelA and the modified red fluorescent protein DsRed-Express (RelA-DsRed-Express). Continual TNFα stimulation elicited oscillations in IκBα-EGFP expression out of phase with the RelA N-C oscillations (Fig. 3, A and B). This caused a statistically significant delay in the timing of nuclear RelA peaks 1, 2, and 3 (Fig. 3F). The amplitude was also slightly reduced for peaks 2 and 3 in the presence of the κB-IκBα-EGFP expression vector (Fig. 3E).

To investigate parameters affecting the oscillation dynamics, we used a computational model (*13*) that predicted NF-κB oscillations with a similar period and damping as those observed here. From this model, we noted that changes in just two molecular species (variables), free IKK and IκBα, were intimately coupled to the oscillation dynamics of nuclear NF-κB (fig. S16). Transfection with the κB-IκBα-EGFP expression vector (Fig. 3, A, B, E, and F) was equivalent to increasing the rate of NF-κB–dependent IκBα transcription; thus, we chose to study the effect of this parameter in the model (reaction 28 in table S1; Fig. 3, C and D; and fig. S17).

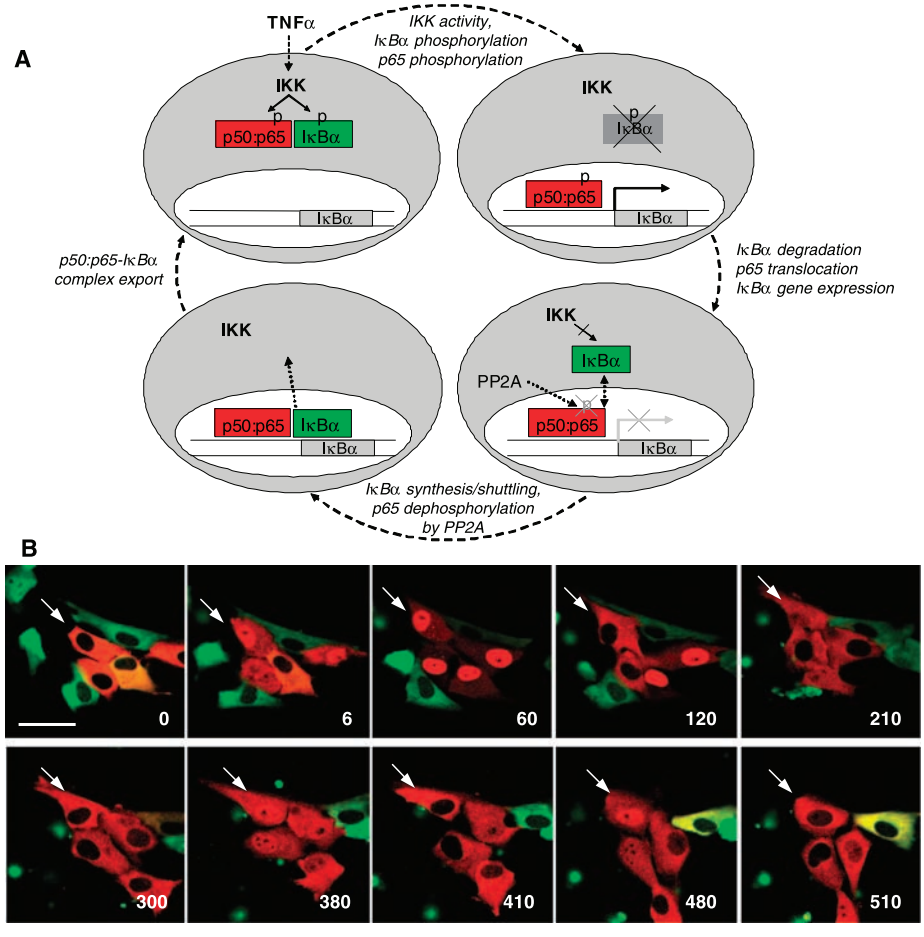

Fig. 1. Oscillations in NF-κB localization. (**A**) Schematic diagram illustrating the potential mechanism for repeated oscillations in NF-κB (p65/RelA) N-C localization. (**B**) Time-lapse confocal images of SK-N-AS cells expressing RelA-DsRed (red) and IκBα-EGFP (green) showing single-cell asynchronous N:C oscillations in RelA-DsRed localization after stimulation with 10 ng/ml TNFα. The arrow marks one oscillating cell. Times, min; scale bar, 50 μm.

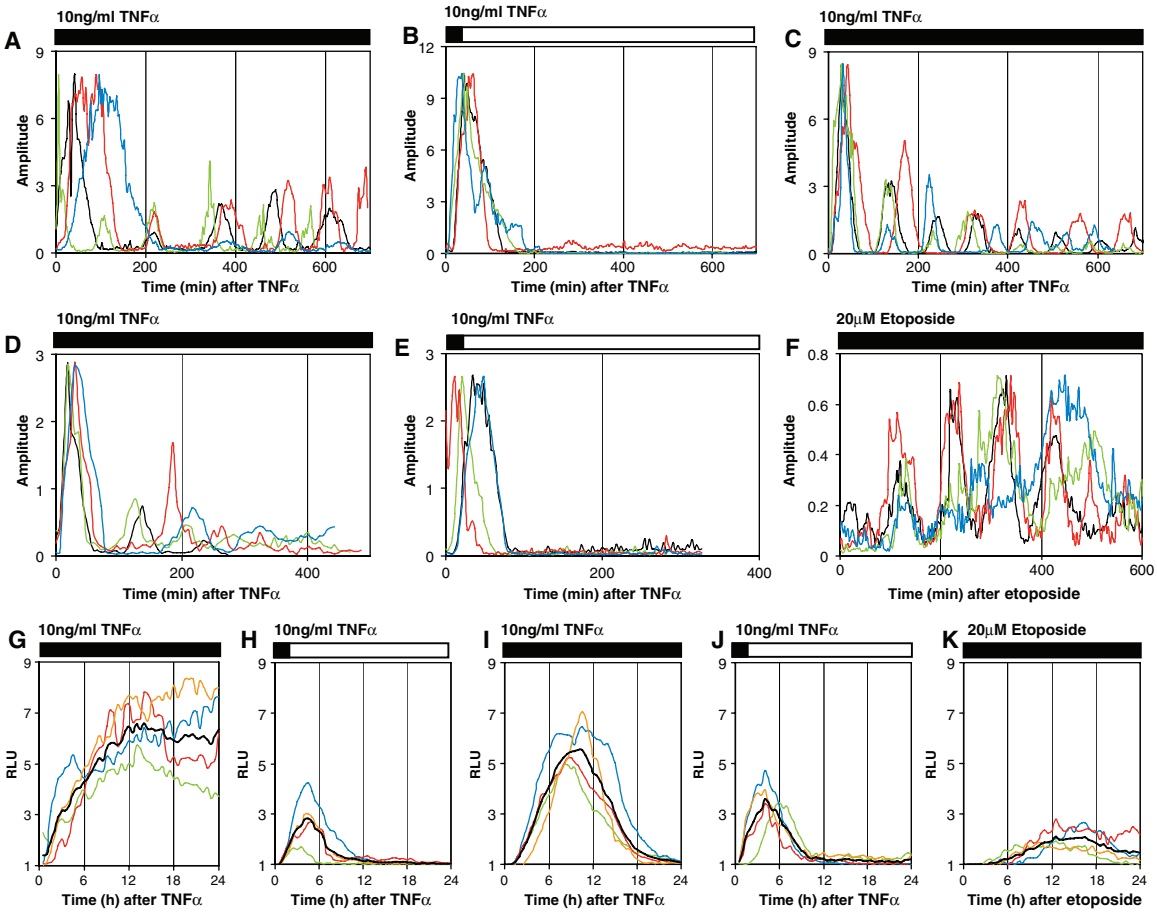

Fig. 2. Analysis of the dynamics of NF-κB localization and κB-dependent reporter gene expression. (**A** to **F**) Time course of N:C localization of RelA-DsRed in cells co-expressing IκBα-EGFP [(A), (B), (D), (E), and (F)] or EGFP control (C). N:C ratio in RelA-DsRed fluorescence was normalized to highest peak intensity. The peak N:C ratio was expressed as the average value for each set of four cells. Data from each cell is represented by a different colored line. (**G** to **K**) Luminescence imaging (RLU, relative light units) of the dynamics of κB-dependent luciferase reporter activity represented as a different colored line for each of four different cells. The black line represents the average of the cells. [(A), (C), and (G)] SK-N-AS cells treated with continual 10 ng/ml TNFα. [(D) and (I)] HeLa cells treated with continual 10 ng/ml TNFα. [(B) and (H)] SK-N-AS cells treated with a 5-min TNFα pulse. [(E) and (J)] HeLa cells treated with a 5-min TNFα pulse. [(F) and (K)] SK-N-AS cells treated with 20 μM of etoposide. The black bar above each graph is a representation of the duration of TNFα treatment. For images of data in [(B) to (F)], (G), and (I), see figs. S6 to S11.

See (*19*) for analysis of some other related parameters (figs. S18 and S19). As the rate of this reaction was increased, there was a delay in simulated peaks 2 and onward (Fig. 3, C, D, and G). Thus, the computational analysis showed the effects of this reaction rate to be similar to those seen in the experimental studies. One discrepancy between the computational model and the experimental data was the unpredicted delay in experimentally observed peak 1 caused by κB-IκBα-EGFP transfection (Fig. 3, F and G). It is unclear how the two cell types studied differ with respect to the values of the parameters used in the model. Given that the oscillations are naturally asynchronous between cells and that this might be associated with varying levels of IκB proteins (*13*) or a lack of optimization of the pre-equilibration step in the model, this may explain why the timing of peak 1 was imperfectly predicted.

The amplitude of oscillations in IκBα-EGFP when expressed under the control of the κB promoter was not directly related to the amplitude of the preceding peak in RelA nuclear localization. In many HeLa cells, peak 2 or 3 in RelA localization was small in amplitude (Fig. 3B) compared with peak 1 (and would not have been observed in asynchronous populations). Nevertheless, these oscillations led to easily observable IκBα-EGFP responses. Thus, persistence of NF-κB oscillations maintains NF-κB–dependent transcription. However, NF-κB translocation cannot be the only factor regulating transcriptional activation (a property of the whole system), and further NF-κB activating and inactivating reactions, including modifications of RelA by phosphorylation (*3*, *4*, *20*), acetylation (*21*), or prolyl isomerization/targeted degradation (*22*), have also been described. The cessation of NF-κB–dependent transcription in the nucleus, independent of nuclear export (*11*), might occur as a consequence of RelA inactivation. Thus, NF-κB oscillations could repeatedly deliver newly activated NF-κB into the nucleus, maintaining a high nuclear ratio of active:inactive NF-κB. To investigate this hypothesis, we used the CRM1-dependent nuclear export inhibitor leptomycin B (LMB) to trap RelA in the nucleus of SK-N-AS cells (Fig. 4, A and B). This resulted in transitory κB-dependent luciferase reporter gene expression (*11*) that peaked after ~5 hours (Fig. 4C). Western blot analysis indicated a transient increase in Ser32 phospho-IκBα expression after 5 min, with no subsequent recovery (Fig. 4E). Ser536 phospho-RelA expression was maximal at 5 min after stimulation and decayed to the threshold of detection by 180 min (in contrast to cells treated with constant TNFα, Fig. 4D). These data support the hypothesis (*23*) that rapid dephosphorylation of NF-κB in the nucleus [by PP2A activity (*24*)] may be a key factor in the switch-off of NF-κB–dependent gene expression.

We propose that oscillations in NF-κB localization coupled to cycles of RelA and IκBα phosphorylation maintain NF-κB–dependent gene expression. Calcium spikes at intervals as long as 30 min have been shown to maintain NF-κB activity in T cells (*25*). The decoding of this [Ca^{2+}] spike frequency might be related to the observed kinetics of oscillatory transcription factor shuttling and regulation (*26*). Specific, non-

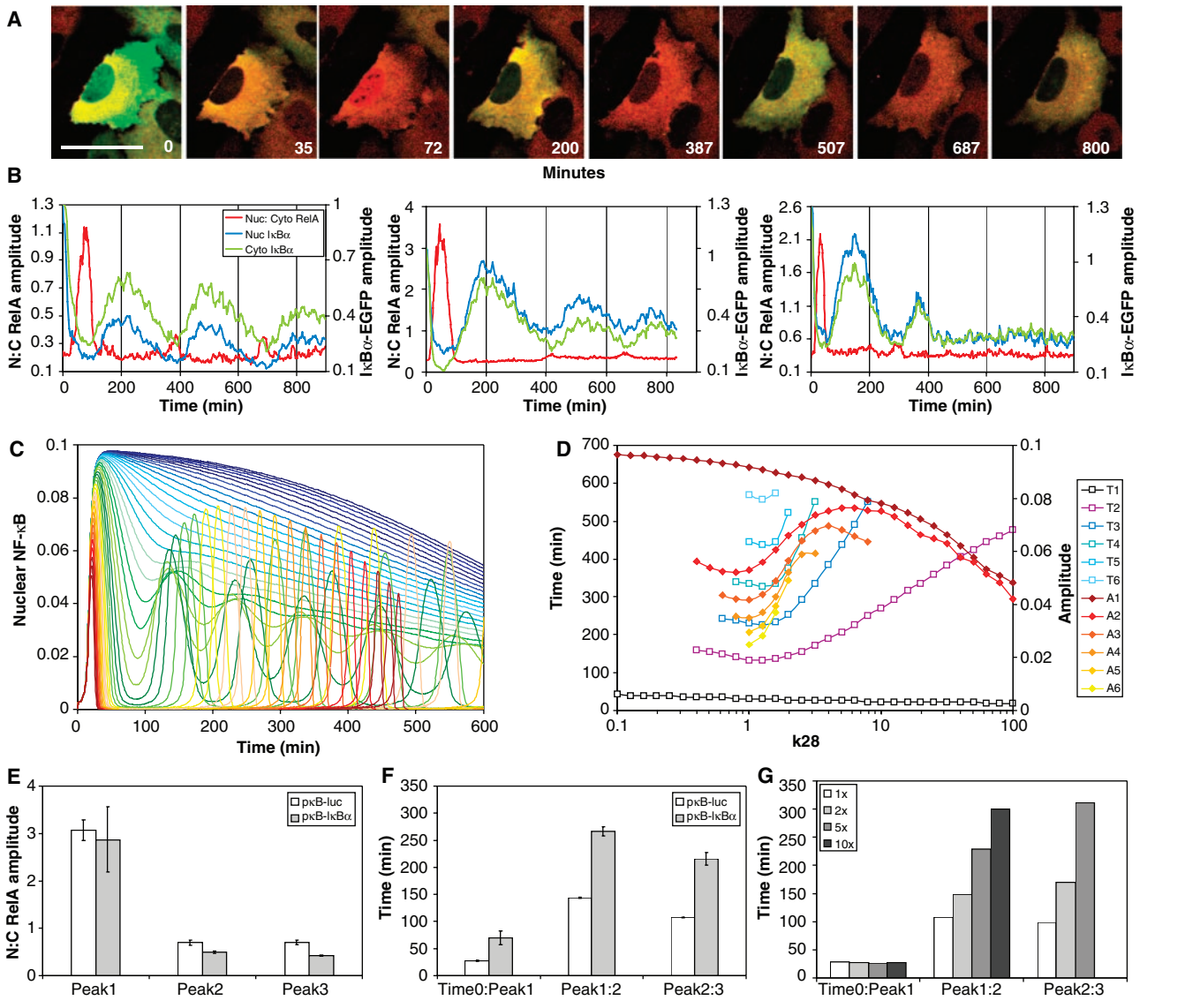

Fig. 3. NF-κB–directed oscillations in IκBα expression. Experimental and computational analysis of factors affecting the amplitude and period of oscillations. (A, B, E, and F) HeLa cells were transfected to express RelA-DsRed-Express and IκBα-EGFP under the control of either the consensus κB promoter or a control κB promoter vector. Cells were stimulated with continual 10 ng/ml TNFα. (**A**) Confocal time course of one typical cell showing oscillations in both RelA-DsRed-Express (red) localization and IκBα-EGFP (green) expression. Scale bar, 50 μm. (**B**) Analysis of three typical cells showing RelA-DsRed-Express N:C ratio and cytoplasmic and nuclear IκBα-EGFP levels. (**C**) The simulated time-dependent nuclear localization of NF-κB for successively increasing the NF-κB–regulated IκBα transcription rate constant by two orders of magnitude on either side of the standard rate constant (reaction 28 in the computational model, table S1) is shown by 41 lines changing in regularly increasing log intervals from blue to green to yellow to red (scanned after equilibration). (**D**) The peak amplitudes (A1 to A6) and timings (T1 to T6) of the first six simulated peaks for different rate constant values for NF-κB regulated IκBα transcription [as determined from data in (C)]. (**E**) Experimentally determined relative amplitude (N:C ratio) of successive RelA-DsRed-Express oscillations in HeLa cells continually stimulated with TNFα. Peak 1 set to 100%; subsequent peaks show relative amplitude ±SEM). (**F**) Average timing between successive peaks (±SEM) of successive N-C oscillations in RelA-DsRed-Express. (**G**) Simulated peak timings for 1x, 2x, 5x, and 10x standard reaction rate constant for NF-κB–regulated IκBα transcription (reaction 28 in computational model, table S1). The parameter was changed before the equilibration period.

linear "network motifs" can decode frequencies rather than amplitudes (*27*). Therefore, the signal-processing elements of the NF-κB signaling pathway, and its interaction with other dynamic signaling systems, may involve the encoding and decoding of specific time-varying signals. Such temporal encoding could avoid undesirable cross talk between cellular signaling pathways that share common components. Furthermore, oscillatory phosphorylation of RelA at Ser536 appears to be a consequence of its shuttling between the cytoplasm and the nucleus. Oscillatory modifications at other regulatory amino acids in RelA (*21*, *28*) might also occur as a consequence of N-C oscillations, whereas changes in N-C oscillation frequency and persistence might explain differential regulation of cell fate in response to different stimuli. Thus, in common, and perhaps in combination, with other oscillatory transcription factor pathways such as p53 (*7*, *8*), NF-κB may constitute a complex analog-to-digital coding system that regulates cell fate.

References and Notes

1. S. Ghosh, M. J. May, E. B. Kopp, *Annu. Rev. Immunol.* **16**, 225 (1998).
2. J. A. DiDonato, M. Hayakawa, D. M. Rothwarf, E. Zandi, M. Karin, *Nature* **388**, 548 (1997).

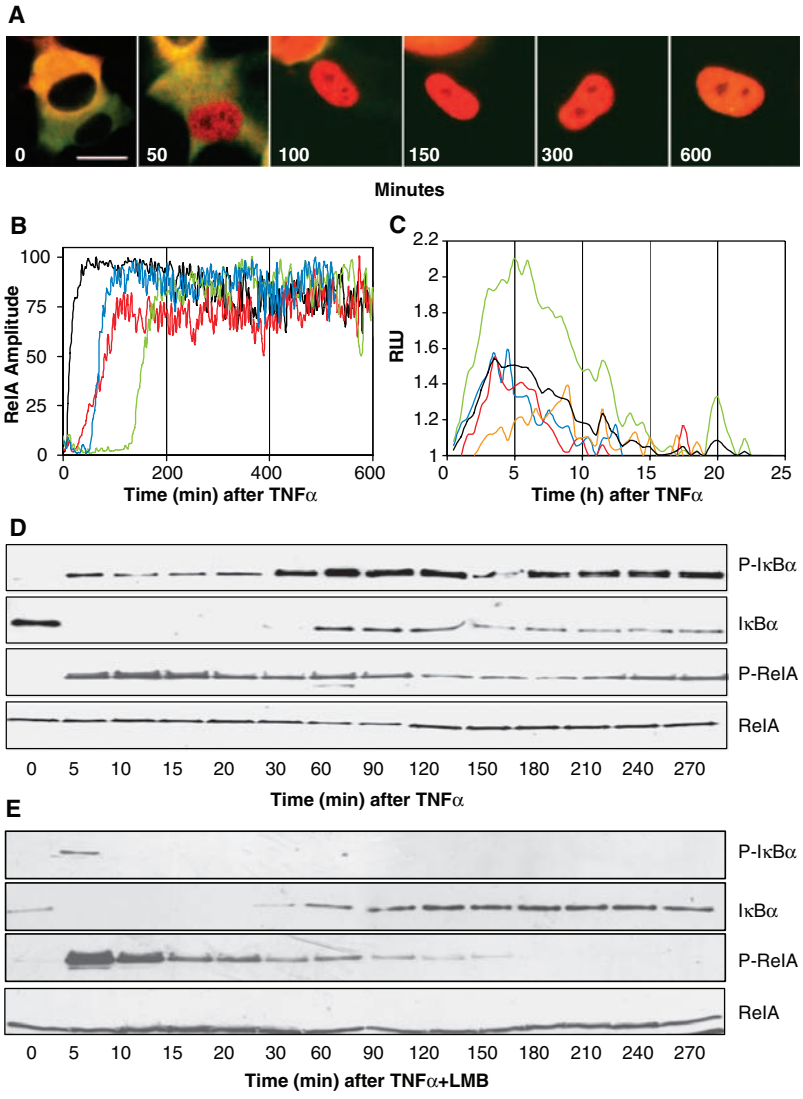

Fig. 4. Effect of nuclear export inhibition on the dynamics of RelA localization, κB-dependent reporter gene expression, and NF-κB phosphoprotein expression. SK-N-AS cells were treated with continuous 10 ng/ml TNFα and 10 ng/ml LMB (unless stated). (**A**) Time-lapse confocal images of RelA-EGFP localization. (**B**) Time course of RelA-EGFP localization expressed as N:C fluorescence ratio (each colored line represents data from one of four single cells). (**C**) κB-dependent luciferase reporter gene expression (each colored line represents data from one of four single cells, and the black line represents the average). (**D**) Western blot analysis of Ser32 phospho-IκBα (P-IκBα), total IκBα (IκBα), Ser536 phospho-RelA (P-RelA), and total RelA (RelA) protein levels in SK-N-AS cells stimulated with continual 10 ng/ml TNFα for the indicated times before analysis. (**E**) Western blot analysis of SK-N-AS cells stimulated with continual 10 ng/ml TNFα and 18 nM LMB for the indicated times before analysis.

3. H. Sakurai, H. Chiba, H. Miyoshi, T. Sugita, W. Toriumi, *J. Biol. Chem.* **274**, 30353 (1999).
4. X. Jiang, N. Takahashi, N. Matsui, T. Tetsuka, T. Okamoto, *J. Biol. Chem.* **278**, 919 (2003).
5. S. C. Sun, P. A. Ganchi, D. W. Ballard, W. C. Greene, *Science* **259**, 1912 (1993).
6. M. W. Young, S. A. Kay, *Nature Rev. Genet.* **2**, 702 (2001).
7. G. Lahav *et al.*, *Nature Genet.* **36**, 147 (2004).
8. N. A. Monk, *Curr. Biol.* **13**, 1409 (2003).
9. O. Pourquié, *Science* **301**, 328 (2003).
10. F. Arenzana-Seisdedos *et al.*, *Mol. Cell. Biol.* **15**, 2689 (1995).
11. G. Nelson *et al.*, *J. Cell Sci.* **115**, 1137 (2002).
12. E. Zandi, Y. Chen, M. Karin, *Science* **281**, 1360 (1998).
13. A. Hoffmann, A. Levchenko, M. L. Scott, D. Baltimore, *Science* **298**, 1241 (2002).
14. A. Y. Ting, D. Endy, *Science* **298**, 1189 (2002).
15. M. J. Berridge, *Nature* **386**, 759 (1997).
16. G. Nelson *et al.*, *J. Cell Sci.* **116**, 2495 (2003).
17. X. Bian *et al.*, *J. Biol. Chem.* **277**, 42144 (2002).
18. D. W. McFerran *et al.*, *Endocrinology* **142**, 3255 (2001).
19. Materials and methods are available as supporting material on *Science* Online.
20. L. Vermeulen, G. De Wilde, S. Notebaert, W. Vanden Berghe, G. Haegeman, *Biochem. Pharmacol.* **64**, 963 (2002).
21. L. Chen, W. Fischle, E. Verdin, W. C. Greene, *Science* **293**, 1653 (2001).
22. A. Ryo *et al.*, *Mol. Cell* **12**, 1413 (2003).
23. H. Sakurai *et al.*, *J. Biol. Chem.* **278**, 36916 (2003).
24. J. Yang, G. H. Fan, B. E. Wadzinski, H. Sakurai, A. Richmond, *J. Biol. Chem.* **276**, 47828 (2001).
25. R. E. Dolmetsch, R. S. Lewis, C. C. Goodnow, J. I. Healy, *Nature* **386**, 855 (1997).
26. R. S. Lewis, *Biochem. Soc. Trans.* **31**, 925 (2003).
27. D. B. Kell, *Curr. Opin. Microbiol.* **7**, 296 (2004).
28. L. F. Chen, W. C. Greene, *J. Mol. Med.* **81**, 549 (2003).

29. This work was supported by the Merseyside Neuroblastoma Research Fund, Alder Hey Oncology Fund, North West Cancer Research Fund, AstraZeneca, Medical Research Council, Department of Trade and Industry, Engineering and Physical Sciences Research Council, Royal Society of Chemistry, Biotechnology and Biological Sciences Research Council, and Pfizer UK. Carl Zeiss, Hamamatsu Photonics, and Kinetic Imaging provided technical support. We thank A. Hoffmann and A. Levchenko for assistance with the NF-κB model and M. Begon, A. Hall, A. Loudon, A. Millar, H. Rees, J. Turnbull, and the late Ray Paton for helpful discussions.

Supporting Online Material

www.sciencemag.org/cgi/content/full/306/5696/704/DC1
Materials and Methods
Figs. S1 to S19
Movies S1 to S4
References

5 May 2004; accepted 11 August 2004